Flow difference effect in the lattice hydrodynamic model*

Tian Jun-Fang(田钧方), Jia Bin(贾 斌)†,
Li Xing-Gang(李新刚), and Gao Zi-You(高自友)

MOE Key Laboratory for Urban Transportation Complex Systems Theory and Technology, Beijing Jiaotong University, Beijing 100044, *China*

(Received 10 August 2009; revised manuscript received 27 September 2009)

In this paper, a new lattice hydrodynamic model based on Nagatani's model [Nagatani T 1998 *Physica* A **261** 599] is presented by introducing the flow difference effect. The stability condition for the new model is obtained by using the linear stability theory. The result shows that considering the flow difference effect leads to stabilization of the system compared with the original lattice hydrodynamic model. The jamming transitions among the freely moving phase, the coexisting phase, and the uniform congested phase are studied by nonlinear analysis. The modified KdV equation near the critical point is derived to describe the traffic jam, and kink–antikink soliton solutions related to the traffic density waves are obtained. The simulation results are consistent with the theoretical analysis for the new model.

Keywords: lattice hydrodynamic model, traffic flow, flow difference

PACC: 0340K, 0570F, 0570J

1. Introduction

In recent years, traffic problems have attracted considerable attention.[1−6] Many traffic models have been proposed by scientists, such as car following models, cellular automata models, gas kinetic models, and hydrodynamic models.[7−29] The transitions from freely moving traffic to jammed traffic have been described in these models. Moreover, the hydrodynamic models and the car following models have been investigated by using linear stability theory and the nonlinear analysis method.[30,31] Also, the lattice hydrodynamic models as a type of hydrodynamic model are convenient for analysing the density waves in traffic flow.

In 1998, Nagatani[22,23] proposed the first lattice hydrodynamic model, which was derived by discretizing the following continuum model:

$$\partial_t \rho + \partial_x(\rho v) = 0, \tag{1}$$

$$\partial_t(\rho v) = a\rho_0 V(\rho(x+\delta)) - a\rho v, \tag{2}$$

where ρ_0 is the average density, and a is the sensitivity of the driver, δ represents the average headway, $\delta = 1/\rho_0$. The $\rho(x+\delta)$ is the local density at position $x+\delta$ at time t, which is related to the inverse of headway $h(x,t)$, i.e. $\rho(x+\delta) = 1/h(x,t)$. $V(\rho(x+\delta))$ is the optimal velocity. The idea is that a driver adjusts the vehicle velocity according to the observed headway $h(x,t)$ or density ahead $\rho(x+\delta)$. This is similar to the idea in the car following models with the optimal velocity $V(h(x,t))$.

Then, for dimensionless space x (let $\widetilde{x} = x/\delta$, and $\widetilde{x}$ is indicated as x hereafter), the lattice model is expressed as

$$\partial_t \rho_j + \rho_0(\rho_j v_j - \rho_{j-1} v_{j-1}) = 0, \tag{3}$$

$$\partial_t(\rho_j v_j) = a\rho_0 V(\rho_{j+1}) - a\rho_j v_j, \tag{4}$$

where j denotes the site on the one-dimensional lattice, and ρ_j and v_j denote the local density and the local average velocity on site j at time t, respectively. The modified KdV equation has been derived and the kink–antikink soliton solution obtained near the critical point in this model.

In 2004, Xue[24] improved Nagatani's lattice model by taking the next-nearest-neighbour lattice site into account. In 2005, Ge[25] proposed an extended lattice model by considering an arbitrary number of front lattice sites. Later, Ge[26] proposed another extended lattice model by incorporating the backward looking effect, and the KdV equation near the neutral stability line is derived. Furthermore, the

*Project supported by the National Basic Research Program of China (Grant No. G2006CB705500), the National Natural Science Foundation of China (Grant Nos. 70501004, 70701004 and 70631001), Program for New Century Excellent Talents in University (Grant No. NCET-07-0057).

†Corresponding author. E-mail: jiabin@jtys.bjtu.edu.cn

© 2010 Chinese Physical Society and IOP Publishing Ltd

lattice models were applied by Nagatani to a two-lane highway and in high-dimensional traffic flow.[27,28]

In this paper, a new model is proposed by considering the flow difference between the leading and following lattices. The linear stability theory is given and the neutral stability condition is obtained. Result shows that the new model could also stabilize the traffic flow. Moreover, we carry out a nonlinear analysis near the neutral stability line. The mKdV equation is derived and the kink–antikink soliton is obtained near the critical point.

This paper is organized as follows: In the following section, the new model is presented. In Section 3, the linear stability analysis is given. In Section 4, the mKdV equation around the critical point is derived by applying the reductive perturbation method. In Section 5, we carry out a simulation to prove our analytical results. Finally, the conclusions are given in Section 6.

2. The new model

On the basis of the lattice model proposed by Nagatani, the flow difference lattice model (FDLM) is presented:

$$\partial_t \rho_j + \rho_0(\rho_j v_j - \rho_{j-1} v_{j-1}) = 0, \tag{5}$$

$$\partial_t(\rho_j v_j) = a\rho_0 V(\rho_{j+1}) - a\rho_j v_j + \lambda(\rho_{j+1} v_{j+1} - \rho_j v_j), \tag{6}$$

where λ is the sensitivity of a driver, and we set a small value of λ (at least $\lambda <= 1$). From the new model, one can see that adjusting the flow of lattice j already takes into consideration not only the density of lattice $j+1$, but also the flow of it.

The flow difference in FDLM is similar to the rule of velocity difference in the FVDM model.[29] By introducing the velocity difference, the stability region of FVDM is bigger than that of the optimal velocity model (OVM),[9] and the vehicle's dynamic behaviours of FVDM are more realistic than that of OVM. In this paper, we will prove that FDLM is also an improvement of Nagatani's model in the following sections. As we know, in real traffic, if the downstream flow is bigger than the upstream flow, generally, it means that the traffic condition of the downstream road is better than that of the upstream road. Thus, the upstream drivers could accelerate, so the flow from upstream to downstream becomes larger. In FDLM, the flow difference could describe this phenomenon to some extent. Moreover, in the same density, the congested traffic on the road may be in a state of the synchronized flow or the wide moving jams, and the flux of the synchronized flow is bigger than that of wide moving jams[3] in the same density. In fact, the flow difference could help distinguish the traffic conditions in the front.

By eliminating speed v in Eqs. (5) and (6), one could obtain the following density equation

$$\partial_t^2 \rho_j + a\rho_0^2(V(\rho_{j+1}) - V(\rho_j)) + a\partial_t \rho_j - \lambda(\partial_t \rho_{j+1} - \partial_t \rho_j) = 0. \tag{7}$$

Moreover, the optimal velocity is chosen as follows:

$$V(\rho) = (v_{\max}/2)[\tanh(1/\rho - h_c) + \tanh(h_c)], \tag{8}$$

where h_c is the safety distance, and the critical density $\rho_c = 1/h_c$. For simplicity, we set $v_{\max} = 2$. It can be seen that the optimal velocity function has the following properties: it is a monotonically decreasing function, it has an upper bound (maximal velocity), and it has a turning point at the safety distance.

3. Linear stability analysis

A linear stability analysis can be conducted for FDLM. It is obvious that the steady state is the uniform traffic flow with a constant density ρ_0 and optimal velocity $V(\rho_0)$. So, the steady-state solution is given by

$$\rho_j(t) = \rho_0, \quad v_j(t) = V(\rho_0). \tag{9}$$

Suppose that $y_j(t)$ is a small deviation from the steady-state density of the vehicle j: $\rho_j(t) = \rho_0 + y_j(t)$, and $y_j(t) = \exp(\mathrm{i}kj + zt)$. Therefore, we obtain

$$V(\rho_j) = V(\rho_0) + V' y_j(t),$$
$$V(\rho_{j+1}) = V(\rho_0) + V' y_{j+1}(t), \tag{10}$$
$$y_{j+1}(t) = y_j(t)\exp(\mathrm{i}k), \quad \partial_t \rho_j = z y_j(t),$$
$$\partial_t \rho_{j+1} = z y_{j+1}(t), \quad \partial_t^2 \rho_j = z^2 y_j(t), \tag{11}$$

where

$$V' = \frac{\mathrm{d}V(\rho)}{\mathrm{d}\rho}\Big|_{\rho=\rho_0}.$$

Substituting Eqs. (10) and (11) into Eq. (7), we have

$$z^2 + a\rho_0^2 V'(\mathrm{e}^{\mathrm{i}k} - 1) + az - \lambda z(\mathrm{e}^{\mathrm{i}k} - 1) = 0. \tag{12}$$

Inserting $z = u\mathrm{i}$ into Eq. (12), with u being a real number, and making its real part and imaginary part equal zero, we obtain

$$-u^2 + a\rho_0^2 V' \cos k - a\rho_0^2 V' - \lambda u \sin k = 0, \tag{13}$$

$$-a\rho_0^2 V' \sin k + au - \lambda u \cos k + \lambda u = 0. \quad (14)$$

From Eq. (14), one can have

$$u = \frac{a\rho_0^2 V' \sin k}{a - \lambda \cos k + \lambda}. \quad (15)$$

Letting $\sigma = a - \lambda \cos k + \lambda$ and substituting Eq. (15) into Eq. (13), we obtain

$$V' = \frac{\lambda a/\sigma - a(\cos k - 1)/\sin^2 k}{-a^2\rho_0^2/\sigma^2}. \quad (16)$$

When $k \to 0$, we then obtain the stability condition

$$a > -2V'\rho_0^2 - 2\lambda. \quad (17)$$

When $\lambda = 0$, we have the stable condition of Nagatani's model

$$a > -2V'\rho_0^2. \quad (18)$$

From Eqs. (17) and (18), one can see that the stability condition can be satisfied in FDLM more easily than in Nagatani's model.

4. Nonlinear stability analysis

We apply the reduction perturbation method to Eq. (7). We introduce slow scales for space variable j and time variable t, and define the slow variables X and T as

$$X = \varepsilon(j + bt), \quad T = \varepsilon^3 t, \quad (19)$$

where b is a constant to be determined later. We set the densities $\rho_j(t)$ to be

$$\rho_j(t) = \rho_c + \varepsilon R(X, T). \quad (20)$$

Expanding each term in Eq. (7) to the fifth order of ε, one obtains

$$\partial_t \rho_j(t) = \varepsilon^2 b \partial_X R + \varepsilon^4 \partial_T R, \quad (21)$$

$$\partial_t^2 \rho_j(t) = \varepsilon^3 b \partial_X^2 R + \varepsilon^5 2b \partial_T \partial_X R, \quad (22)$$

$$\rho_{j+1}(t) = \rho_c + \varepsilon R + \varepsilon^2 \partial_X R + \frac{1}{2}\varepsilon^3 \partial_X^2 R + \frac{1}{6}\varepsilon^4 \partial_X^3 R + \frac{1}{24}\varepsilon^5 \partial_X^4 R, \quad (23)$$

$$V(\rho_{j+1}) = V(\rho_c) + V'(\rho_c)(\rho_{j+1} - \rho_c) + \frac{1}{6}V'''(\rho_c)(\rho_{j+1} - \rho_c)^3, \quad (24)$$

$$\begin{aligned} & V(\rho_{j+1}) - V(\rho_j) \\ &= V'(\rho_c)\varepsilon^2 \partial_X R + \frac{V'(\rho_c)}{2}\varepsilon^3 \partial_X^2 R \\ &\quad + \frac{V'(\rho_c)}{6}\varepsilon^4 \partial_X^3 R + \frac{V'(\rho_c)}{24}\varepsilon^5 \partial_X^4 R \\ &\quad + \frac{V'''(\rho_c)}{6}\varepsilon^4 \partial_X R^3 + \frac{V'''(\rho_c)}{12}\varepsilon^5 \partial_X^2 R^3, \end{aligned} \quad (25)$$

$$\begin{aligned} & \partial_t \rho_{j+1}(t) - \partial_t \rho_j(t) \\ &= \varepsilon^3 b \partial_X^2 R + \varepsilon^5 \partial_T \partial_X R + \frac{1}{2}\varepsilon^4 b \partial_X^3 R \\ &\quad + \frac{1}{6}\varepsilon^5 b \partial_X^4 R. \end{aligned} \quad (26)$$

Substituting Eqs. (21)–(26) into Eq. (7), we obtain the following expression:

$$\begin{aligned} & \varepsilon^2(a\rho_c^2 V'(\rho_c) + ab)\partial_X R + \varepsilon^3 \left(b^2 + \frac{a\rho_c^2 V'(\rho_c)}{2} - \lambda b\right)\partial_X^2 R \\ & + \varepsilon^4 \left(\frac{a\rho_c^2 V'(\rho_c)}{6}\partial_X^3 R + \frac{a\rho_c^2 V'''(\rho_c)}{6}\partial_X R^3 - \frac{\lambda b}{2}\partial_X^3 R + a\partial_T R\right) \\ & + \varepsilon^5 \left((2b - \lambda)\partial_T \partial_X R + \left(\frac{a\rho_c^2 V'(\rho_c)}{24} - \frac{\lambda b}{6}\right)\partial_X^4 R + \frac{a\rho_c^2 V'''(\rho_c)}{12}\partial_X^2 R^3\right) = 0. \end{aligned} \quad (27)$$

Near the critical point, we have (ρ_c, a_c), $a_c = a(1 + \varepsilon^2)$. By taking $b = -\rho_c^2 V'(\rho_c)$ and eliminating the second and third order terms of Eq. (27), we obtain the simplified equation

$$\varepsilon^4[\partial_T R - g_1 \partial_X^3 R + g_2 \partial_X R^3] + \varepsilon^5[g_3 \partial_X^2 R + g_4 \partial_X^4 R + g_5 \partial_X^2 R^3] = 0, \quad (28)$$

where

$$g_1 = \frac{\lambda b}{2a_c} - \frac{\rho_c^2 V'(\rho_c)}{6}, \quad g_2 = \frac{\rho_c^2 V'''(\rho_c)}{6}, \quad g_3 = \frac{b(b - \lambda)}{a_c},$$

$$g_4 = \frac{2b - \lambda}{a_c}\left(\frac{\lambda b}{2a_c} - \frac{\rho_c^2 V'(\rho_c)}{6}\right) + \frac{\rho_c^2 V'(\rho_c)}{24} - \frac{\lambda b}{6a_c}, \quad g_5 = \frac{\rho_c^2 V'''(\rho_c)}{12} - \frac{(2b - \lambda)\rho_c^2 V'''(\rho_c)}{6a_c}.$$

In order to derive the standard mKdV equation, we make the following transformations:

$$T' = g_1 T, \quad R = \sqrt{\frac{g_1}{g_2}} R'.$$

So, equation (28) turns into

$$\partial_{T'} R' - \partial_X^3 R' + \partial_X R'^3 + \varepsilon M[R'] = 0, \tag{29}$$

where

$$M[R'] = \sqrt{\frac{1}{g_1}} \left(g_3 \partial_X^2 R' + \frac{g_1 g_5}{g_2} \partial_X^2 R'^3 + g_4 \partial_X^4 R' \right).$$

Equation (29) is the mKdV equation with an $O(\varepsilon)$ correction term. We ignore the $O(\varepsilon)$ term and obtain the mKdV equation with the kink–antikink soliton solution

$$R_0'(X, T') = \sqrt{c} \tanh \left[\sqrt{\frac{c}{2}} (X - cT') \right]. \tag{30}$$

Supposing $R'(X, T') = R_0'(X, T') + \varepsilon R_1'(X, T')$, in order to determine the value of the propagation velocity for the kink–antikink soliton solution, it is necessary to satisfy the following condition

$$(R_0', M[R_0']) \equiv \int_{-\infty}^{+\infty} \mathrm{d}X R_0' M[R_0'] = 0 \tag{31}$$

with $M[R_0'] = M[R']$. By solving Eq. (31), we obtain the selected value c[31]

$$c = \frac{5 g_2 g_3}{2 g_2 g_4 - 3 g_1 g_5}. \tag{32}$$

Hence, we obtain the kink–antikink soliton solution ($-\rho_c^2 V' = 1, \rho_c^6 V''' = 2$)

$$\rho_j = \rho_c + \varepsilon \sqrt{\frac{g_1 c}{g_2}} \tanh \left(\sqrt{\frac{c}{2}} (X - c g_1 T) \right) \tag{33}$$

with $\varepsilon^2 = a_c/a - 1$. The amplitude A of the solution is

$$A = \sqrt{\frac{g_1}{g_2} \varepsilon^2 c}. \tag{34}$$

The kink–antikink solution represents the coexisting phase, which includes both freely moving phase and jamming phase. The density of the freely moving phase is given by $\Delta x = \rho_c + A$. The density of the jamming phase is given by $\Delta x = \rho_c - A$.[27] Then, we obtain the coexisting curve in the headway-sensitivity space.

Figure 1 shows the coexisting curves and the neutral stability curves in the density-sensitivity space. For each pair of curves, the space is divided into three regions, i.e. the stable region, the metastable region and the unstable region. In the stable region, the traffic flow is stable. In the metastable and unstable region, a small disturbance will lead to the congested traffic. It can be seen that with the increase of λ, the unstable region will reduce. The limit case of $\lambda = 0$ corresponds to Nagatani's model.

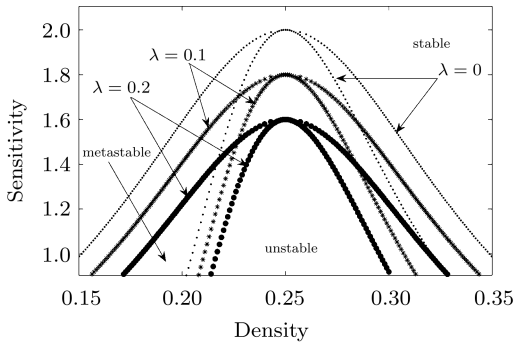


Fig. 1. Phase diagram in the density-sensitivity space. The neutral stability curves are given by Eq. (17). The space is divided into three regions by the neutral stability curve and coexisting stability curve: stable region, metastable region and unstable region ($V_{\max} = 2, h_c = 4$).

5. Simulation

For the convenience of simulation, we rewrite Eq. (7) into the difference form

$$\begin{aligned} &\rho_j(t + 2\tau) - \rho_j(t + \tau) + \tau \rho_0^2 (V(\rho_{j+1}(t)) \\ &- V(\rho_j(t))) - \tau\lambda(\rho_{j+1}(t + \tau) - \rho_{j+1}(t) \\ &- \rho_j(t + \tau) + \rho_j(t)) = 0. \end{aligned} \tag{35}$$

The initial conditions of the numerical simulation are set as follows: There are $L = 100$ lattices in the system, and the periodical boundary condition is applied. The densities of every lattice are set to be $\rho_j(0) = 0.25$, $\rho_j(1) = 0.25$ for $j \neq 49$ and 50, $\rho_j(1) = 0.3$ for $j = 49$, $\rho_j(1) = 0.2$ for $j = 50$; $\tau = 1/a = 1$, $\rho_0 = \rho_c = 0.25$. Simulation results are shown in Fig. 2. Firstly, the kink–antikink soliton solutions are depicted in Fig. 2, because the stability condition is unsatisfied. Secondly, the amplitudes of the density waves decrease with the increase of λ. Note that the smaller the amplitude is, the better the stability of the traffic flow is. Therefore, through the analytical and simulation results, we can conclude that a traffic jam can be suppressed more effectively by taking the flow difference into account.

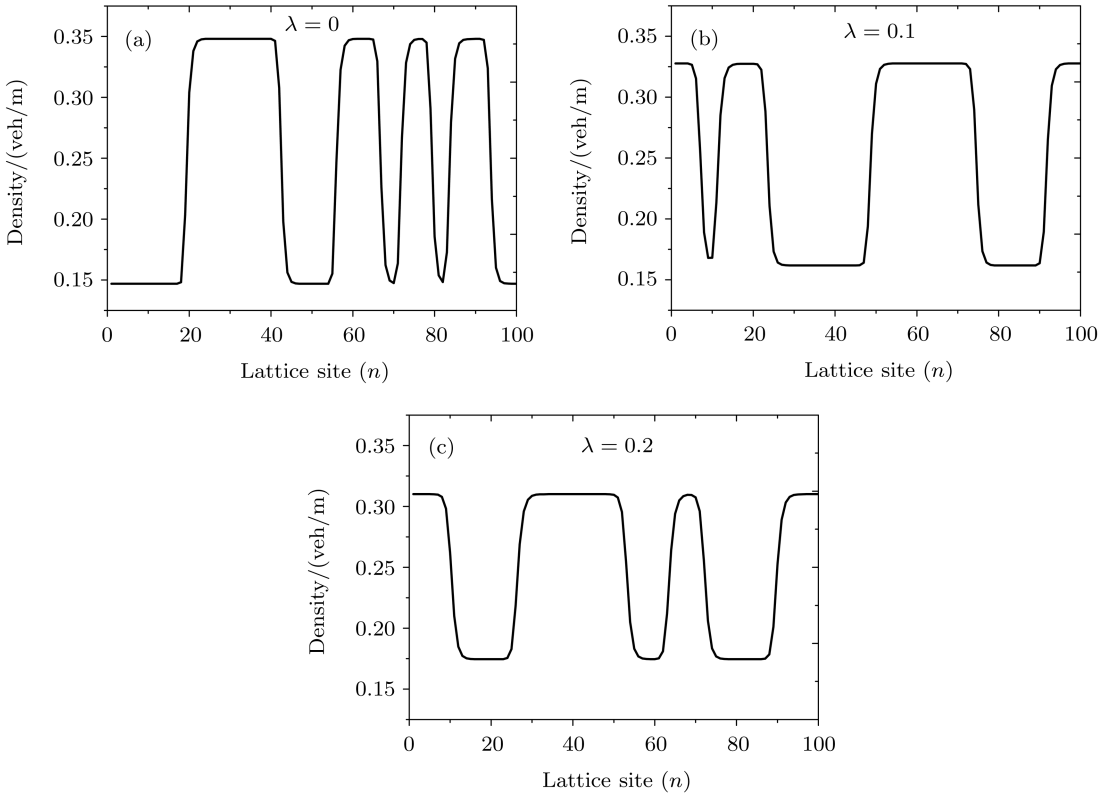


Fig. 2. The densities of all lattices for different values of λ.

6. Conclusions

We have proposed a new lattice traffic model in order to suppress traffic jams. We have investigated the traffic behaviours by the use of linear stability theory and nonlinear wave analysis. We derived the modified KdV equation to describe the traffic jam near the critical point and obtained the kink–antikink soliton solutions related to the traffic density waves. Phase diagrams in the density-sensitivity space with the neutral stability curves and the coexisting curves are given for different values of sensitivity λ. It can be seen that when we increase the value of λ, the unstable region will reduce. The results show that the flow difference effect plays an important role in stabilising the traffic flow. The simulation results are consistent with the theoretical analysis for the new model.

References

[1] Chowdhury D, Santen L and Schadschneider A 2000 *Phys. Rep.* **329** 199
[2] Helbing D 2001 *Rev. Mod. Phys.* **73** 1067
[3] Kerner B S 2004 *The Physics of Traffic* (Heidelberg: Springer)
[4] Nagatani T 2002 *Rep. Prog. Phys.* **65** 1331
[5] Helbing D 2000 *Traffic and Granular Flow* **99** (Heidelberg: Springer)
[6] Jia B, Gao Z Y, Li K P and Li X G 2007 *Models and Simulations of Traffic System Based on the Theory of Cellular Automaton* (Beijing: Science Press)
[7] Herman R, Montrol E W, Potts R B and Rothery R W 1959 *Oper. Res.* **7** 86
[8] Newell G F 1961 *Oper. Res.* **9** 209
[9] Bando M, Hasebe K, Nakayama A, Shibata A and Sugiyama Y 1995 *Phys. Rev.* E **51** 1035
[10] Treiber M, Hennecke A and Helbing D 2000 *Phys. Rev.* E **62** 1805
[11] Nagel K and Schreckenberg M 1992 *J. Phys.* A **2** 2221
[12] Li X B, Wu Q S and Jiang R 2001 *Phys. Rev.* E **64** 066128
[13] Jiang R and Wu Q S 2003 *J. Phys.* A: *Math. Gen.* **36** 381
[14] Kerner B S, Klenov L S and Wolf D E 2002 *J. Phys.* A: *Math. Gen.* **35** 9971
[15] Prigogine I and Herman R 1971 *Kinetic of Vehicular Traffic* (New York: Elsevier)
[16] Helbing D 1996 *Phys. Rev.* E **53** 2366
[17] Kerner B S and Konhauser P 1993 *Phys. Rev.* E **48** 2335
[18] Ge H X, Zhu H B and Dai S Q 2005 *Acta Phys. Sin.* **54** 4621 (in Chinese)

[19] Wang T, Gao Z Y and Zhao X M 2006 *Acta Phys. Sin.* **55** 634 (in Chinese)
[20] Li K P, Gao Z Y and Mao B H 2007 *Chin. Phys.* **16** 359
[21] Xue Y 2002 *Chin. Phys.* **11** 1128
[22] Nagatani T 1998 *Physica* A **261** 599
[23] Nagatani T 1999 *Physica* A **264** 581
[24] Xue Y 2004 *Acta Phys. Sin.* **53** 25 (in Chinese)
[25] Ge H X, Dai S Q, Xue Y and Dong L Y 2005 *Phys. Rev.* E **71** 066119
[26] Nagatani T and Cheng R J 2008 *Physica* A **387** 6952
[27] Nagatani T 1999 *Physica* A **265** 297
[28] Nagatani T 1999 *Physica* A **272** 592
[29] Jiang R, Wu Q S and Zhu Z J 2001 *Phys. Rev.* E **64** 017101
[30] Kurtze D A and Hong D C 1995 *Phys. Rev.* E **52** 218
[31] Komatsu T and Sasa S 1995 *Phys. Rev.* E **52** 5574
[32] Ge H X, Cheng R J and Dai S Q 2005 *Physica* A **357** 466